mol) and glycine (2.25 g, 0.03 mol) were combined with 50 ml of DMF in 150 ml of dry benzene. Nitrogen gas was used to flush a system consisting of the reaction flask with contents, a Dean-Stark trap filled with benzene, and a water-cooled condenser before starting the reaction by heating the heterogeneous benzene suspension. After 2 hr, about 0.6 ml of water had been collected (theoretical 0.54 g). The hot solution was filtered under nitrogen to give a clear light yellowish filtrate. Some crystallization took place on cooling. The solution was concentrated on a rotary evaporator, and the crystals were filtered under nitrogen and washed with petroleum ether (80% yield).

Tributyltin Glycinate. Bis(tributyltin) oxide (4.25 g, 0.01 mol) and glycine (1.50 g, 0.02 mol) were combined with 7 ml of DMF in 150 ml of benzene. The reaction was carried out as described above. After 4 hr 0.19 ml of water had been collected (theoretical 0.18 g). The hot solution was filtered under nitrogen, and benzene was evaporated on a rotary evaporator. The small amount of solid formed in the remaining DMF solution was filtered and washed with petroleum ether (35% yield).

Tricyclohexyltin Glycinate. DMF was not used in this synthesis. Following a similar procedure as above, tricyclohexyltin hydroxide (0.02 mol) and glycine (0.02 mol) gave water (0.33 ml; theoretical 0.36 ml) and the product in 48% yield after 6 hr.

Deuteration of Glycine. Glycine (*ca.* 5 g) was dissolved in 99.8% D_2O in a stoppered flask and left at room temperature for 1 month. Addition of excess acetone precipitated the deuterated glycine (94% yield).

Deuteration of L-α-Isoleucine. Isoleucine (2.7 g) was partially dissolved in 99.8% D_2O at room temperature, left for 2 weeks in a stoppered flask, and then warmed for 2 days during which time all solids dissolved. Crystallization took place on cooling. The remaining deuterium oxide was evaporated *in vacuo* to yield the deuterated isoleucine (2.6 g).

Bis(tricyclohexyltin) Carbonate. Tricyclohexyltin hydroxide (1 g) was dissolved in 100 ml of dry benzene, and carbon dioxide was bubbled through the solution overnight. Bis(tricyclohexyltin) carbonate (mp 195–197°) remained after the solvent was evaporated. *Anal.* Calcd: C, 55.80; H, 8.36; Sn, 29.81. Found: C, 54.80; H, 8.38; Sn, 29.69.

Bis(trimethyltin) Carbonate. Carbon dioxide was bubbled overnight through a solution of trimethyltin hydroxide (1 g) in 100 ml of benzene. The solid isolated was infusable above 210° (lit.[42] mp >200°).

(42) H. Sato, *Bull. Chem. Soc. Jap.*, **40**, 410 (1967).

The amino acid and dipeptide derivatives studied were purified by recrystallization from hot benzene solution, except the following compounds which were purified by sublimination: trimethyltin glycinate, trimethyltin glycylglycinate, and tributyltin glycinate (sublimed using a cold finger at −78° with a maximum oil bath temperature of 150, 165, and 160, respectively, under a pressure of 0.1, 0.005, and 0.02 Torr, respectively).

The single crystals of trimethyltin glycinate used for X-ray study were grown by sublimation using a pointed cold finger kept at −78° with an oil bath temperature of 140–150° and at a pressure of 90 Torr.

Registry No. Trimethyltin hydroxide, 39700-41-9; tricyclohexyltin hydroxide, 39700-42-0; bis(tributyltin)oxide, 56-35-9; glycine, 56-40-6; DL-alanine, 302-72-7; DL-α-aminobutyric acid, 2835-81-6; DL-valine, 516-06-3; DL-leucine, 328-39-2; L-isoleucine, 73-32-5; β-alanine, 107-95-9; glycylglycine, 556-50-3; Me_3Sn(gly), 39700-30-6; Me_3Sn(ala), 39700-31-7; Me_3Sn(but), 39700-32-8; Me_3Sn(val), 39700-33-9; Me_3Sn(leu), 39700-34-0; Me_3Sn(isoleu), 39700-35-1; Me_3Sn(β-ala), 39700-36-2; Me_3Sn(glygly), 39700-37-3; Bu_3Sn(gly), 39700-38-4; Cyh_3Sn(gly), 39700-39-5; Cyh_3Sn(ala), 39699-39-3; Cyh_3Sn(but), 39678-69-8; Cyh_3Sn(val), 39678-70-1; Cyh_3Sn(leu), 39699-40-6; Cyh_3Sn(isoleu), 39699-41-7; Cyh_3Sn(β-ala), 39700-40-8; Cyh_3Sn(glygly), 39708-58-2; bis(tricyclohexyltin) carbonate, 39678-71-2; bis(trimethyltin) carbonate, 16469-60-6; carbon dioxide, 124-38-9.

Acknowledgment. Our work is supported by the National Science Foundation through Grant No. GP-16,544. We thank Professors G. J. Janz and S. C. Wait and Dr. K. B. Subrahmanyam of the Rensselaer Polytechnic Institute, Troy, N. Y., for help in obtaining the laser Raman spectra, Professor G. A. Eadon of SUNY–Albany for help with obtaining the mass spectra, Professor N. W. G. Debye for helpful discussions, and the M and T Chemicals Co. for kindly supplying some of the tin starting materials.

Contribution from the Research Laboratories, Eastman Kodak Company, Rochester, New York 14650

Electron Paramagnetic Resonance Investigations of Photosensitive Transition Metal Oxalates. Copper-Doped $K_2Pd(C_2O_4)_2 \cdot 2H_2O$

R. S. EACHUS* and W. G. McDUGLE

Received November 20, 1972

In a general study of photosensitive materials, an epr investigation of a single crystal of $K_2Pd(C_2O_4)_2 \cdot 2H_2O$ substitutionally doped with the paramagnetic cupric ion has been carried out at ambient temperature. The magnetic data were analyzed using a spin Hamiltonian which included the quadrupole term. An evaluation of the bonding parameters for the included copper complex revealed that in the ground state the unpaired electron is confined to the $d_{x^2-y^2}$ metal orbital. However, in the excited state there is significant delocalization of unpaired electron density into the oxalate ligand π orbitals. A mechanism for the observed photoconductivity of the host material is proposed.

Introduction

Some interest has been shown recently in the solid-state photochemistry of transition metal–oxalate complexes.[1-4] Potassium bis(oxalato)palladium(II) dihydrate (KOPD) is known to be photosensitive and the following overall reaction scheme has been proposed to account for the formation of aggregated palladium atoms during exposure of the solid material[5]

$$n K_2Pd(C_2O_4)_2 \cdot 2H_2O \xrightarrow[300^\circ K]{h\nu} Pd^\circ{}_n + 2nCO_2 + 2nH_2O + nK_2C_2O_4$$

(1) H. E. Spencer and M. W. Schmidt, *J. Phys. Chem.*, **74**, 3472 (1970).
(2) H. E. Spencer, *J. Phys. Chem.*, **73**, 2316 (1969).
(3) H. E. Spencer and M. W. Schmidt, *J. Phys. Chem.*, **75**, 2986 (1971).
(4) W. G. McDugle, Abstracts, 164th National Meeting of the American Chemical Society, New York, N. Y., 1972, No. INOR 67.
(5) H. E. Spencer and J. E. Hill, *Photogr. Sci. Eng.*, **16**, 234 (1972).

In this process the quantum yield for formation of carbon dioxide is reported to be 0.02 ± 0.01 at 366 nm.[5]

The primary aim of the present study was to elucidate the mechanisms of photodecomposition in crystalline KOPD. The most reasonable initial step upon irradiation of the material involves the photoproduction of an electron-hole pair, the electron being trapped by the divalent palladium ion and the hole trapped by one of the oxalate ligands producing Pd^+ and an oxalate radical, respectively. One of several events would then occur: (1) recombination, (2) transfer of another electron from the oxalate radical to the palladium to which it was previously coordinated, forming CO_2 and Pd^0, and (3) the intermolecular diffusion of an electron to some distant trapping site such as a palladium ion or another oxalate radical, resulting in recombination. Recombination is certainly the most important event, as evidenced by the low quantum yield. If the intermolecular diffusion of an electron is the favored event leading to a photochemical reaction, there may be a preferential pathway for electron transmission through the crystalline material, which would agree with the observed photoconductivity.[5]

Our initial studies involved irradiating single crystals of pure KOPD at various temperatures between 77°K and ambient in an attempt to detect paramagnetic intermediates in the photoreaction by epr spectroscopy. At temperatures below approximately 150°K the material was inherently stable to all radiation wavelengths between 250 and 600 nm. Above this temperature the oxalate complex was so sensitive that photodecomposition occurred almost instantaneously under illumination with 366-nm radiation. We could detect no paramagnetic intermediates by this approach. Consequently, we incorporated minute quantities of the cupric complex $K_2Cu(C_2O_4)_2 \cdot 2H_2O$ into KOPD as a structural probe. The Cu^{2+} ion was selected as the dopant for the following reasons. (a) This ion ($3d^9$), being inherently paramagnetic, would act as a probe of the transition metal ion environment both before photolysis and during exposure. (b) The reduction of Pd^{2+} to atomic palladium presumably goes *via* the monovalent ion, which is also a d^9 species. The included cupric ion should, therefore, experience an environment identical with that of Pd^+ complexes generated by random electron trapping at $[Pd(C_2O_4)_2]^{2-}$ anions.

This report outlines the results of our initial investigations of the KOPD-Cu^{2+} system. It includes a description of the ground-state wave function of the dopant complex, some conclusions regarding the photoconductivity of the host material, and a tentative mechanism for the photoinduced decomposition of KOPD.

Experimental Section

Sample Preparation. Single crystals of potassium bis(oxalato)-palladium(II) dihydrate were grown by controlled evaporation from a saturated aqueous solution. Crystals of $K_2Pd(C_2O_4)_2 \cdot 2H_2O$ are monoclinic (space group $P2_1/n$) with $a = 11.03$, $b = 14.86$, $c = 3.70$ Å, $\beta = 93.8°$, and $Z = 2$.

Samples substitutionally doped with the cupric ion were grown from solutions containing approximately 3% $K_2Cu(C_2O_4)_2 \cdot 2H_2O$. The inclusion of as much as 1000 ppm of the cupric complex had little or no effect upon the crystal structure of the host material. The copper concentrations were determined by atomic absorption spectroscopy. An X-ray diffraction study of a doped crystal yielded crystallographic data that were identical with those previously reported for pure KOPD.[6] Typical crystals were red-brown and had a characteristic needlelike form. Samples suitable for epr measurements (0.5 × 0.5 × 4.0 mm) were accurately mounted onto a quartz rectangular prism, prior to investigation, to facilitate their handling. In samples examined, the elongated c axis lay parallel to the longest axis of the prism and the [110] face was in contact with this quartz support. The principal crystallographic directions were determined by X-ray techniques.

Epr Measurements. Epr spectra were measured on a Varian E-12 spectrometer operating at a nominal frequency of 9.3 GHz. The spectrometer incorporated a commercially available variable-temperature accessory and a liquid helium transfer refrigerator (Air Products and Chemicals, Inc.). Some measurements were made at 77 and 4.2°K with these accessories. Epr rotations were performed about the elongated c axis and orthogonal directions, labeled a' and b', which lay approximately 45° from a^* and b, respectively. The directions a^*, b, and c also defined an orthogonal set with a^* 3.8° ($\beta - 90°$) from a.

Results

The characteristic angular dependencies of the Cu^{2+} epr spectra were monitored as the magnetic field (H_0) was rotated in turn about the elongated crystallographic c axis and the orthogonal directions, a' and b'. Figure 1 shows a typical first-derivative single-crystal spectrum of $K_2Pd(C_2O_4)_2 \cdot 2H_2O$-$Cu^{2+}$ measured with H_0 in the $a'c$ plane.

Essentially, there are 16 intense features in the spectrum. Copper has two magnetic isotopes in natural abundance (^{63}Cu, nuclear spin $I = 3/2$; 69.09% abundant; ^{65}Cu, $I = 3/2$, 30.91% abundant). Consequently, since we expect to get $(2I + 1)$ lines from each isotope, a typical Cu(II) spectrum would be composed of eight lines. A cursory examination of the crystal structure of KOPD[6] (Figure 2) reveals that there are two unique molecular sites per unit cell, which are spatially equivalent only along the a^*, b, and c axes. Consequently, there are 2 × 8 lines from the substitutional cupric complex. In first order, the four lines arising from one ^{63}Cu nucleus in a single crystallographic site would be equally spaced in field. At most orientations of the crystal this is indeed what we observed. However, at positions which were close to the planes of $[Cu(C_2O_4)_2]^{2-}$ complexes, the separations were not equal and it became apparent that there must be a significant quadrupole interaction. The normally "forbidden" epr transitions attained a significant intensity in the region θ = 60-90° (θ is the angle between H_0 and the c axis) and often complicated the analysis of spectra in the region perpendicular to c. These features are marked with dashed lines in Figure 1.

An analysis of the spectra obtained by rotations about a', b', and c indicated that the principal axes of the hyperfine coupling and g tensors were spatially coincident and that these directions were not along the a^*, b, and c axes. To aid our analysis of the experimental results we measured spectra along the principal magnetic axes of the Cu^{2+} complexes. By assuming the radicals to be axially symmetric and applying the well-known expressions derived by Bleaney[7] for such a system, we were able to calculate approximately the parameters $A_\parallel$, $A_\perp$, Q', $g_\parallel$, and $g_\perp$. These values, when substituted into a computational procedure (FIELDS) supplied by Dr. J. A. Hebden of the University of British Columbia, were used to obtain the accurate magnetic data.[8] To illustrate the accuracy of this procedure the angular variation of the hyperfine features in the a^*b plane is displayed in Figure 3. The solid lines are the computer fit of the spin Hamiltonian

$$\mathcal{H} = \beta \mathbf{H} \cdot \mathbf{g} \cdot \mathbf{S} + \mathbf{S} \cdot \mathbf{A} \cdot \mathbf{I} - g_N \beta_N \mathbf{H} \cdot \mathbf{I} + Q'[I_z^2 - 1/3 I(I+1)] \quad (1)$$

(in the usual notation) to the experimental data. For the sake of clarity, we have omitted the angular variations of the forbidden transitions from this figure. These lines were detectable in those regions where the overlap of signals from the two Cu^{2+} sites greatly complicated the spectra.

(6) K. Krogmann, *Z. Anorg. Allg. Chem.*, **346**, 188 (1966).

(7) B. Bleaney, *Phil. Mag.*, **42**, 441 (1951).

(8) C. R. Byfleet, D. P. Chong, J. A. Hebden, and C. A. McDowell, *J. Magn. Resonance*, **2**, 69 (1970).

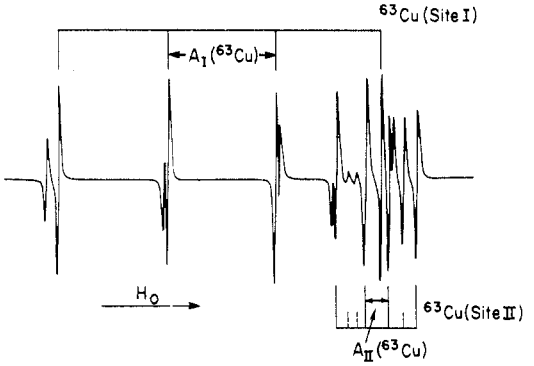

Figure 1. A first-derivative epr spectrum of Cu^{2+}-$K_2Pd(C_2O_4)_2 \cdot 2H_2O$ measured at 77°K with H_0 in the $a'c$ plane.

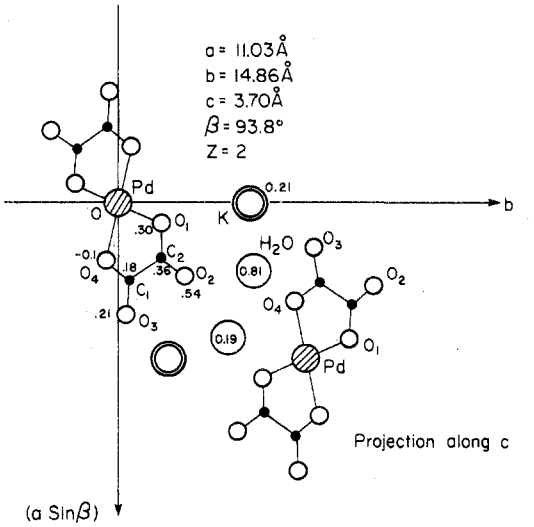

Figure 2. The crystal structure of KOPD projected onto the a^*b plane. Only two water molecules and potassium ions are included.

The phenomenological parameters are given in Table I. Also included in this table are the Euler angles which relate the magnetic axes of the cupric complex to the crystallographic (reference) frame. The signs of A_x, A_y, and Q' relative to A_z can occasionally be obtained from measurements made in high (10,000 G) magnetic fields or, under favorable conditions, they may be deduced from the asymmetry of the forbidden transitions in those orientations where these features are most intense. In the present investigation these transitions were readily observed in the region perpendicular to c and their asymmetric spacing and intensity suggest A_x and A_y have the opposite sign to Q'.[9] Since the nuclear quadrupole term is positive for the majority of cupric complexes, A_x and A_y are taken to be negative.[9] The sign of A_z is also negative and this is in accord with the system under investigation.

When samples of the doped compound were cooled to 4.2°K, we detected very little change in the epr spectrum of the included cupric ion. A large, but not unexpected, line width reduction had little effect on the magnetic data of the dopant. Confirmation of our analysis was obtained from measurements made on polycrystalline samples of this material.

When single-crystal specimens of the Cu^{2+}-doped oxalate were subjected to several instantaneous exposures of 366-nm radiation, they darkened markedly. Furthermore, the epr spectra of the crystalline samples changed significantly. Each hyperfine feature of the original Cu^{2+} spectra was gradually replaced by a small doublet centered upon the field position of the parent resonance. We have been unable to complete our analysis of these spectra because of their complexity at positions where the hyperfine splitting was a minimum.

We can make a tentative assignment, however, and we prefer to associate the observed spectra with a single Cu^{2+}-containing photoproduct occupying four magnetically inequivalent sites per unit cell of KOPD.

Theoretical and Bonding Parameters

The estimation of bonding parameters from epr spin-Hamiltonian data is well established and a comprehensive review has been presented by McGarvey.[10] For such an analysis we require a knowledge of the ground-state wave function, electronic spectra, and molecular structure of the complex in question, in addition to the epr parameters. With this in mind, we shall discuss the probable ground state for the cupric ion in potassium bis(oxalato)palladium(II) dihydrate, retaining throughout the concept of a positive hole.

The cupric complex is almost certainly distorted from perfect D_{4h} symmetry in this environment. In Figure 2, the angle O_4-Pd-O_1 is less than 90° and the substitutional Cu^{2+} dopant is expected to experience this distortion. The overall point group symmetry is most probably D_{2h} and the g and hyperfine coupling tensors included in Table I are in accord with this assignment.

Hitchman[11] has recently used simple crystal-field theory to analyze the g tensors characterizing low-symmetry d^9 metal complexes. Following this analysis, we have found for Cu^{2+} in $K_2Pd(C_2O_4)_2 \cdot 2H_2O$ that the principal values of the hyperfine coupling and g tensors are spatially coincident and that they lie close to the Cu-O bond directions. In such a situation, assuming that the complex has D_{2h} symmetry, the only d states admixed by the ligand field are $|x^2 - y^2\rangle$ and $|3z^2 - r^2\rangle$, so that the ground state can be written as

$$\Psi = a|x^2 - y^2\rangle - b|3z^2 - r^2\rangle$$

where $a^2 + b^2 = 1$. We have calculated a^2 and b^2 to be 0.999 and 0.001, respectively. This value of b^2 is negligibly small so that the $|3z^2 - r^2\rangle$ d-orbital contribution to the ground-state wave function has been neglected in the proceeding calculations of the bonding parameters.

Under this condition the cupric complex can be assumed to have D_{4h} point symmetry, a good approximation considering the close similarity of g_x to g_y and A_x to A_y (see Table I). The antibonding molecular orbitals for a Cu^{2+} ion surrounded by a square-planar arrangement of oxygen atoms are, in the probable order of increasing energy

$$e_g = \begin{cases} \beta d_{xz} - \dfrac{\beta'}{\sqrt{2}}\chi_{e_g}(\pi_1) \\ \beta d_{yz} - \dfrac{\beta'}{\sqrt{2}}\chi_{e_g}(\pi_2) \end{cases}$$

$$b_{2g} = \gamma d_{xy} - \frac{\gamma'}{2}\chi_{b_{2g}}(\pi_3)$$

$$a_{1g} = n d_{3z^2-r^2} - \frac{n'}{2}\chi_{a_{1g}}(\sigma) \qquad (2)$$

$$b_{1g} = \alpha d_{x^2-y^2} - \frac{\alpha'}{2}\chi_{b_{1g}}(\sigma)$$

where $\chi_\Gamma(\sigma,\pi)$ designates a symmetry-adapted σ or π linear combination of the ligand orbitals belonging to the Γ irreduc-

(9) H. So and R. Linn Belford, *J. Amer. Chem. Soc.*, 91, 2392 (1969).

(10) B. R. McGarvey, *Transition Metal Chem.*, 3, 90 (1966).

(11) M. A. Hitchman, *J. Chem. Soc. A*, 4 (1970).

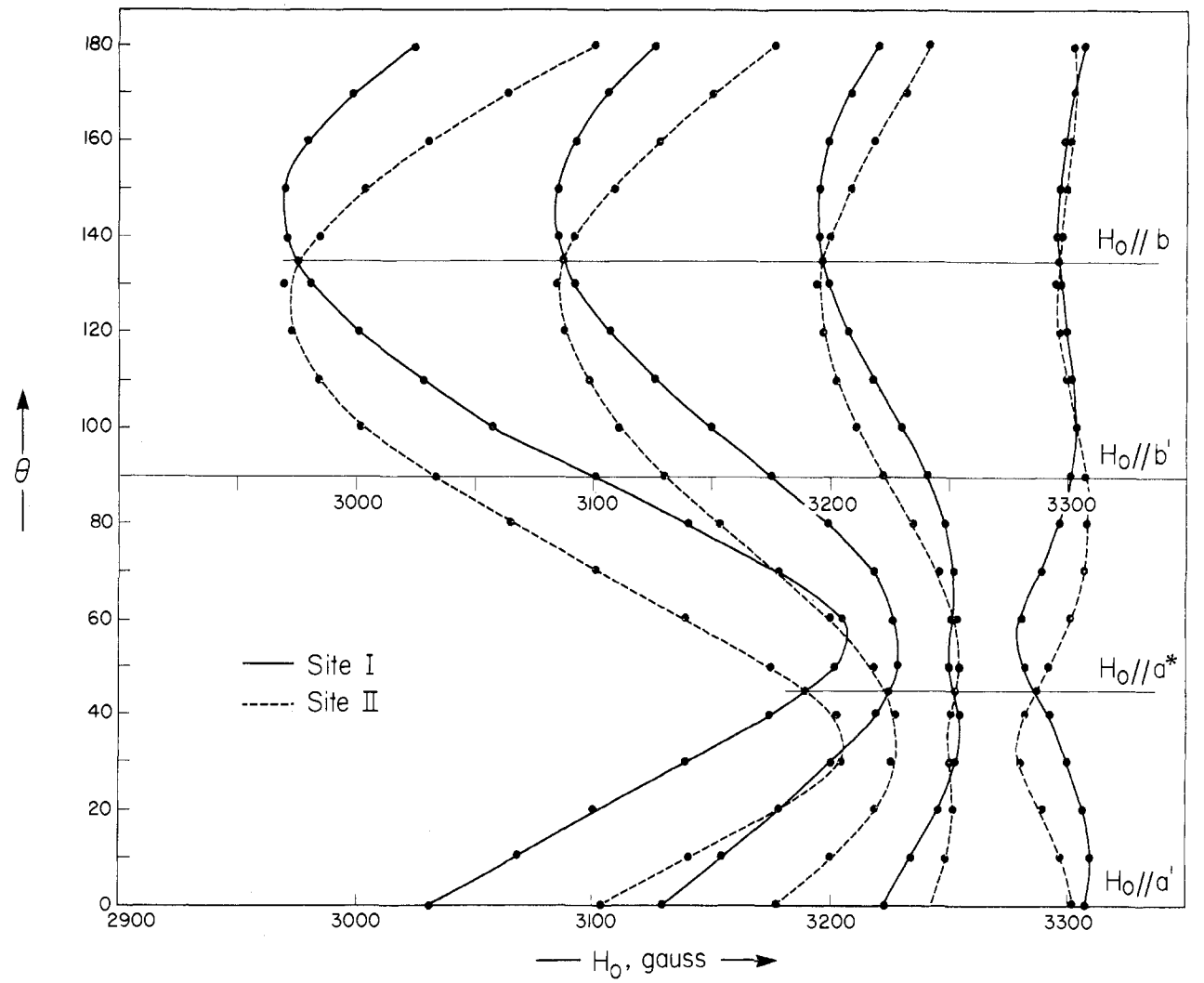

Figure 3. The angular dependencies of the $^{63}Cu^{2+}$ spectra in the a^*b plane: •, experimental points; full and dashed lines, computed best-fit data.

Table I. Magnetic Parameters for Cu^{II}-$K_2Pd(C_2O_4)_2 \cdot 2H_2O$ at 300°K

g Tensor	^{63}Cu hyperfine tensor × 10^4, cm^{-1}	Direction cosines with respect to a^*	b	c	$10^4Q'$, cm^{-1}
$g_x = 2.0595$	$A_x = -15.0$	−0.980	0.210	0.000	
$g_y = 2.0560$	$A_y = -20.0$	0.175	0.820	0.550	
$g_z = 2.2815$	$A_z = -181.1$	0.113	−0.533	−0.840	(+)4.1

ible representation of the D_{4h} point group and the unpaired electron is confined to the b_{1g} antibonding orbital. If we make the approximation that all overlap between the ligand and metal orbitals can be neglected, except that between $d_{x^2-y^2}$ and the oxygen σ orbitals, the following expressions for the g-tensor elements can be derived[12]

$$g_z = g_\parallel = g_e - \frac{8\lambda_0\alpha^2\gamma^2}{\Delta E(\parallel)} + \frac{8\lambda_0\alpha\gamma}{\Delta E(\parallel)}\left\{\alpha'\gamma S + \frac{\alpha'}{2}(1-\gamma^2)^{1/2}T(r)\right\} \quad (3)$$

$$g_x = g_y = g_\perp = g_e - \frac{2\lambda_0\alpha^2\beta^2}{\Delta E(\perp)} + \frac{2\lambda_0\alpha\beta}{\Delta E(\perp)}\left\{\alpha'\beta S + \frac{\alpha'}{\sqrt{2}}(1-\beta^2)^{1/2}T(r)\right\} \quad (4)$$

where $\Delta E(\parallel) = E(b_{2g}) - E(b_{1g})$ and $\Delta E(\perp) = E(e_g) - E(b_{1g})$.

(12) D. Kivelson and R. Neimen, *J. Chem. Phys.*, **35**, 149 (1961).

Furthermore, we can express the principal values of the hyperfine coupling tensor in the form

$$A_z = A_\parallel = -\frac{4}{7}\alpha^2P - K + \Delta g_\parallel P + \frac{3}{7}\Delta g_\perp P - \frac{6\lambda_0\alpha\beta}{7\Delta E(\perp)}\left\{\alpha'\beta S + \frac{\alpha'}{\sqrt{2}}(1-\beta^2)^{1/2}T(r)\right\} - \frac{8\lambda_0\alpha\gamma}{\Delta E(\parallel)}\left\{\alpha'\gamma S + \frac{\alpha'}{2}(1-\gamma^2)^{1/2}T(r)\right\} \quad (5)$$

$$A_x = A_y = A_\perp = +\frac{2}{7}\alpha^2P - K + \frac{11}{14}\Delta g_\perp P - \frac{22\lambda_0\alpha\beta}{14\Delta E(\perp)}\left\{\alpha'\beta S + \frac{\alpha'}{\sqrt{2}}(1-\beta^2)^{1/2}T(r)\right\} \quad (6)$$

where (i) $\Delta g_\parallel = g_\parallel - g_e$ and $\Delta g_\perp = g_\perp - g_e$, (ii) $P = g_e g_N \beta_e \beta_N \langle r^{-3}\rangle$, and (iii) K is the isotropic (Fermi) contact term.

Equations 5-8 were solved using the values $P = 360 \times 10^{-4}$ cm^{-1} and $\lambda_0 = -828$ cm^{-1} for the basic parameters[10] and applying a simple iterative technique in which the terms in α' were treated as correction factors. The question of the energy difference $\Delta E(\parallel)$ and $\Delta E(\perp)$ now arises. It is usual to obtain these from the electronic spectrum of the paramagnetic complex in question. The electronic spectrum of pure $K_2Cu(C_2O_4)_2 \cdot 2H_2O$ consists of one very broad band centered at 14,800 cm^{-1}. Since the half-width of this line is approx-

imately 3000 cm^{-1}, we have assumed that the components of this band lie at approximately 14,000 and 16,000 cm^{-1}, which we have assigned to $\Delta E(\parallel)$ and $\Delta E(\perp)$, respectively.[13] We have also assumed that on doping $[Cu(C_2O_4)_2]^{2-}$ into its palladium analog, no change in its electronic spectrum occurs.

The values of K, α^2, β^2, and γ^2 determined from this analysis are collated in Table II. The value of K has been used to compute the quantity χ given by

$$\chi = \frac{4\pi}{S}\left(\Psi\left|\sum_i \delta(r_i) S_{zi}\right|\Psi\right) = -\frac{3}{2}\left(\frac{hca_0^3}{g_e g_N \beta_e \beta_N}\right) K \text{ au} \quad (7)$$

χ is defined as an effective electron density at the nucleus in question, which is responsible for an isotropic contribution to the hyperfine interaction tensor. Electrons in d orbitals cannot contribute directly to χ, but finite values of this parameter result from a polarization of the inner filled s orbitals by the unpaired d electrons. A typical value of χ for Cu^{2+} in a square-planar oxygen environment is -3.6 ± 0.4 au.[14] We have calculated χ to be -3.81 au for the Cu^{2+} ion in KOPD. If we reexpress eq 3 and 4 in the forms

$$g_\parallel = g_e - \frac{8\lambda_0 k_\parallel^2}{\Delta E_\parallel} \quad (8)$$

$$g_\perp = g_e - \frac{2\lambda_0 k_\perp^2}{\Delta E_\perp} \quad (9)$$

where $k_\parallel^2$ and $k_\perp^2$ are as defined in ref 15, we can compute the orbital-reduction factors ($k_\parallel$ and $k_\perp$) of the system in question. These parameters are usually employed to estimate covalency and the values obtained for $[Cu(C_2O_4)_2]^{2-}$ were $k_\parallel = 0.77$ and $k_\perp = 0.73$.

Discussion

A paramagnetic dopant $K_2Cu(C_2O_4)_2 \cdot 2H_2O$ has been employed to probe the palladium environment in single crystals of $K_2Pd(C_2O_4)_2 \cdot 2H_2O$ using epr techniques. Although the crystal structure of $K_2Cu(C_2O_4)_2 \cdot 2H_2O$ is triclinic and different from that of the monoclinic KOPD, analysis of the angular variations of the copper hyperfine and g tensors reveals that the copper is present substitutionally in the host. The concentration of copper in the samples studied was approximately 100 ppm, *i.e.*, sufficiently dilute that the nearest-neighbor metal ions were palladium. Because of the fact that the crystal structures of $K_2Cu(C_2O_4)_2 \cdot 2H_2O$ and KOPD are so different, it is doubtful that a sufficiently high concentration of the copper complex could be doped into the palladium host to bring about electron exchange between adjacent copper centers. Doped single crystals grown from aqueous solutions containing as high as 20% $K_2Cu(C_2O_4)_2 \cdot 2H_2O$ contained only 1000 ppm of the cupric complex.

A detailed analysis of the epr data places the unpaired electron in the b_{1g} ($3d_{x^2-y^2}$) copper orbital in the ground state. The small anisotropy in the g_x and g_y tensor elements reflects a very small amount of copper $3d_{3z^2-r^2}$ admixture into the b_{1g} molecular orbital, indicating that the unpaired electron is predominantly in the plane of the copper complex. A low value of approximately 0.18 for α'^2 (eq 3-6) places a small amount of unpaired electron density into the b_{1g} ligand orbitals. The most probable ordering of the highest filled and lowest partially filled molecular orbitals for the dopant $K_2Cu(C_2O_4)_2 \cdot 2H_2O$ having the B_{1g} ground state is $b_{1g} > a_{1g} > b_{2g} > e_g$.

Table II. Bonding Parameters

10^4K, cm^{-1}	α^2	γ^2	β^2
121.0	0.82	0.87	0.73

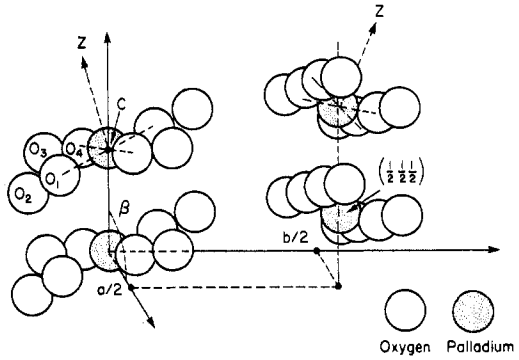

Figure 4. The stacking of the individual oxalate complexes in KOPD. The K^+ ions, H_2O molecules, and carbon atoms have been omitted for clarity.

A careful investigation of the KOPD crystal structure shows that planar $[Pd(C_2O_4)_2]^{2-}$ units are stacked in chains along the c axis (Figure 4). The planes are tilted with respect to c, however, such that the palladium ion of one planar complex lies between the oxalate ligands of the neighboring molecules. Potassium cations and the water molecules lie between the chains and tend to isolate them from each other. This stacking precludes any direct metal-metal′ orbital overlap but still permits interaction between neighboring $[Pd(C_2O_4)_2]^{2-}$ units. This interaction, except for interruptions due to lattice defects, may be extended along the c axis through (metal-ligand-metal′-ligand′-metal″-ligand″) overlap; *i.e.*, a band is formed along the c axis from the appropriate metal and out-of-plane ligand orbitals. Pure KOPD has been observed to be photoconductive,[5] implying the existence and mobility of charge carriers in the excited state. Such a band could be the pathway for movement of charge carriers and would imply that the photoconductivity is for the greater part parallel to the c axis than perpendicular to it.

In the ground state of the copper-doped KOPD and in pure KOPD there is no direct pathway for unpaired electron density to be delocalized into the ligand π orbitals and, therefore, no intermolecular transfer of charge carriers to neighboring groups. The values listed in Table II for the squares of the orbital coefficients β^2 and γ^2 would imply a small but significant amount of unpaired-electron density in the ligand π orbitals contributing to the B_{2g} and E_g excited states of the copper complex. Such covalency is also reflected in the low values of the orbital reduction parameters $k_\parallel$ and $k_\perp$. In the pure host material, the photoconduction process may be viewed as the transfer of unpaired-electron density to the ligand π orbitals through intramolecular photoexcitation and the intermolecular transfer of the carrier by the interaction of metal and ligand π orbitals.

The degree of overlap between a metal ion and its neighboring oxalate ligand is, therefore, very important for the conduction process. Although copper serves as a good paramagnetic probe, it could well hinder the conduction process, for copper 3d orbitals are located closer to the nucleus than are the 4d palladium orbitals. This should reduce the metal-adjacent ligand interaction and adversely affect conduction.

(13) B. N. Figgis, M. Gerloch, J. Lewis, and R. C. Slade, *J. Chem. Soc. A*, 2028 (1968).
(14) B. M. McGarvey, *J. Phys. Chem.*, 71, 51 (1967).
(15) M. A. Hitchman and R. L. Belford, "Electron Spin Resonance of Metal Complexes," T. F. Yen, Ed., Plenum Press, New York, N. Y., 1969.

On the other hand, platinum 5d orbitals project further into space than palladium 4d orbitals. Therefore, one would predict that substitution of KOPD with the analogous platinum salt should increase the degree of metal-adjacent ligand overlap and, consequently, result in an increase in the mobility of the charge carrier in the host.

From the initial photolysis results it appears that reduction of Cu^{2+} does not occur at those metal ions positioned adjacent to the photodecomposed oxalate ligands. We base this conclusion on the fact that we could detect no apparent reduction in the total epr signal intensity from the Cu^{2+} ions during exposure. However, we did note that the Cu^{2+} spectra were modified as the photolysis proceeded. The end product of this exposure was probably CuC_2O_4 isolated in the KOPD environment. This photodecomposition of a single, coordinated oxalate ligand at each impurity-ion site would account for the detection of four magnetically inequivalent sites per unit cell occupied by the cupric ion product. The photoproduced electron must be transmitted through the KOPD crystal to be trapped at a distant $[Pd(C_2O_4)_2]^{2-}$ complex or a lattice defect.

To simplify the task of analysis we are now attempting to follow the photolysis of single crystals of KOPD containing minute quantities of ^{63}Cu (99%). Isotopic enrichment will halve the number of hyperfine lines originating from the copper-containing decomposition products, which should facilitate a complete spectral analysis.

Registry No. $K_2Pd(C_2O_4)_2 \cdot 2H_2O$, 36425-78-2; copper, 7440-50-8.

Contribution from the Department of Chemistry,
University of Western Ontario, London, Ontario, Canada

Chemistry of Metal Hydrides. XV. Mechanism of Double-Bond Migration Induced by Platinum(II) Hydrides

H. C. CLARK* and H. KUROSAWA

Received November 30, 1972

The mechanism of double-bond migration induced by some platinum(II)-hydrido complexes has been investigated using platinum(II)-deuterido analogs as well as 2-deuterated allyl methyl ether. Both the stoichiometric reaction of diallyl ether with Pt–H and the catalytic conversion of allyl alkyl ethers with Pt–H to *cis*-propenyl alkyl ethers were found to involve the initial reversible anti-Markownikov addition of Pt–H across the terminal C=C bond before double-bond migration occurs. Double-bond migration may be achieved through attack by hydridic hydrogen on the terminal carbon and elimination by platinum of another hydrogen atom from allylic carbon. The reaction of butene-1 with Pt–H proceeded similarly.

Introduction

Some transition metal complexes are known to catalyze the migration of C=C bonds in olefinic compounds. Several mechanisms have been proposed[1] to account for this homogeneously catalyzed isomerization, although no single mechanism fully explains all aspects of systems with different transition metal complexes. One of the simplest mechanisms suggested involves the reversible addition of the M–H bond across C=C, so that the formation of the metal hydride and of the hydrido(π-olefinic) complex may well be key steps in the overall reaction

$$-\underset{\text{MH}}{\overset{|}{\underset{|}{\text{CH}}}}=\text{CH}-\text{CH}_2- \rightleftarrows -\text{CH}_2-\underset{\text{M}}{\overset{|}{\underset{|}{\text{CH}}}}-\text{CH}_2- \rightleftarrows -\text{CH}_2-\underset{\text{MH}}{\overset{|}{\underset{|}{\text{CH}}}}=\text{CH}- \qquad (1)$$

We have previously discussed[2] the facile insertion of olefins into the Pt–H bond, in which the formation of the four-coordinate intermediate *trans*-$[PtH(PR_3)_2(\text{olefin})]^+$ from coordinatively unsaturated platinum(II)-hydrido complexes plays an essential role. In extending these studies, we found[3] that double-bond migration and insertion take place readily in the stoichiometric reactions of allylic derivatives with such reactive platinum(II) hydrides as *trans*-$[PtH(PR_3)_2(\text{acetone})]^+$ and *trans*-$PtH(ClO_4)(PPh_3)_2$. More generally, these reactive platinum(II) hydrides were found to be capable of catalyzing the isomerization of butene-1, allyl methyl ether, and allyl phenyl ether at ambient conditions. The present paper describes a series of experiments on both the stoichiometric and the catalytic isomerization of some allylic compounds with platinum-hydrido complexes involving 2-deuterated allyl methyl ether as well as platinum(II)-deuterido complexes. Our results are consistent, in part, with the mechanism proposed by Cramer and Lindsey,[4] who suggested that the isomerization of olefins with platinum(II) complexes involves both Markownikov and anti-Markownikov addition of Pt–H across the terminal C=C bond.

Results and Discussion

Reaction of *trans*-$PtDX(PR_3)_2$ with $(CH_2=CHCH_2)_2O$. In a previous paper,[3] we suggested that the sequence 2 was involved in the reaction of some platinum(II)-hydrido complexes with allylic ethers. *trans*-$PtD(ClO_4)(PPh_3)_2$ (IId) and *trans*-$PtD(NO_3)(PPh_2Me)_2$ (IIId) have now been used with $(CH_2=CHCH_2)_2O$ in order to investigate the mechanism of the isomerization process. In both reactions, the deuterium distribution in the reaction product, CH_3CH_2CHO, was determined from the proton nmr and mass spectra of the 2,4-dinitrophenylhydrazone adduct[5] of propionaldehyde (Table I).

Anti-Markownikov addition of Pt–D across the terminal C=C bond (k_2) (see Scheme I) and reversible elimination of

(1) See, for example, R. S. Coffey, "Aspects of Homogeneous Catalysis," Vol. 1, R. Ugo, Ed., Manfredi, Milan, 1970, p 1; F. R. Hartley, *Chem. Rev.*, 69, 799 (1969), especially p 838.
(2) H. C. Clark and H. Kurosawa, *Inorg. Chem.*, 11, 1275 (1972).
(3) H. C. Clark and H. Kurosawa, *Chem. Commun.*, 150 (1972); *Inorg. Chem.*, 12, 357 (1973).
(4) R. Cramer and R. V. Lindsey, Jr., *J. Amer. Chem. Soc.*, 88, 3534 (1966).